Astron. Astrophys. 347, 518–523 (1999)

ASTRONOMY AND ASTROPHYSICS

X-ray and radio observations of RX J1826.2−1450/LS 5039

M. Ribó[1], **P. Reig**[2,3], **J. Martí**[4], **and J.M. Paredes**[1]

[1] Departament d'Astronomia i Meteorologia, Universitat de Barcelona, Av. Diagonal 647, E-08028 Barcelona, Spain
[2] Physics Department, University of Crete, P.O. Box 2208, GR-71003, Heraklion, Greece
[3] Foundation for Research and Technology-Hellas, GR-71110, Heraklion, Crete, Greece
[4] Departamento de Física, Escuela Politécnica Superior, Universidad de Jaén, Calle Virgen de la Cabeza, 2, E-23071 Jaén, Spain

Received 10 February 1999 / Accepted 19 May 1999

Abstract. RX J1826.2−1450/LS 5039 has been recently proposed to be a radio emitting high mass X-ray binary. In this paper, we present an analysis of its X-ray timing and spectroscopic properties using different instruments on board the RXTE satellite. The timing analysis indicates the absence of pulsed or periodic emission on time scales of 0.02–2000 s and 2–200 d, respectively. The source spectrum is well represented by a power-law model, plus a Gaussian component describing a strong iron line at 6.6 keV. Significant emission is seen up to 30 keV, and no exponential cut-off at high energy is required. We also study the radio properties of the system according to the GBI-NASA Monitoring Program. RX J1826.2−1450/LS 5039 continues to display moderate radio variability with a clearly non-thermal spectral index. No strong radio outbursts have been detected after several months.

Key words: stars: individual: RX J1826.2-1450; LS 5039; NVSS J182614-145054 – stars: variables: general – radio continuum: stars – X-rays: stars

1. Introduction

The star LS 5039 is the most likely optical counterpart to the X-ray source RX J1826.2−1450. Such an association was originally proposed by Motch et al. (1997), hereafter M97, as a result of a systematic cross-correlation between the ROSAT All Sky Survey (Voges et al. 1996) and several OB star catalogues in the SIMBAD database. The unabsorbed X-ray luminosity, at an estimated distance of 3.1 kpc, amounts to $L_{\rm X}$(0.1–2.4 keV) $\sim 8.1\times10^{33}$ erg s^{-1}, and the hardness of the source is well consistent with a neutron star or a black hole, accreting directly from the companion's wind (M97). In the optical, LS 5039 appears as a bright $V \sim 11.2$ star with an O7 V((f)) spectral type. Based on this evidence, M97 proposed the system to be a high mass X-ray binary (HMXRB).

In addition, this system has been found to be active at radio wavelengths. Its radio counterpart (NVSS J182614−145054) is a bright, compact and moderately variable radio source in excellent sub-arcsecond agreement with the optical star (Martí et al. 1998). All these facts point to the peculiar nature of RX J1826.2−1450/LS 5039, and suggest a classification among the selected group of radio emitting HMXRB.

In order to explore how this source behaves compared to other members of its class (e.g. Cygnus X-1, LS I+61°303 and SS 433), we have analyzed the corresponding X-ray data from the All Sky Monitor (ASM) and the Proportional Counter Array (PCA) on board the satellite Rossi X-ray Timing Explorer (RXTE). In Sect. 2 we present an X-ray timing analysis based on both the ASM and the PCA instruments. The ASM data are suitable to study the long-term (days to months) temporal behavior of the source, whereas X-ray variability on shorter time scales (seconds to hours) is better investigated with the PCA. In Sect. 3 a PCA spectroscopic analysis is presented, with the different spectral models that fit the data being examined and discussed.

In the radio domain, RX J1826.2−1450/LS 5039 was included at our request in the list of radio sources routinely monitored at the Green Bank Interferometer (GBI)[1]. At the time of writing, the radio light curves cover $\sim$ 4 months of observations. In Sect. 4 we present the GBI radio data so far acquired with some discussion on the source variability and spectral index properties. Finally, we conclude in Sect. 5 with a brief comparative discussion of RX J1826.2−1450/LS 5039 versus other radio loud HMXRB.

Hereafter, we will refer to the source as RX J1826.2−1450 when discussing the X-rays. In the optical/radio context the LS 5039 designation will be preferred.

2. X-ray timing analysis

2.1. The ASM/RXTE data

The ASM database analyzed in this paper spans for more than two and a half years (1996 February–1998 November) and contains nearly 800 daily flux measurements in the energy range 1.5–12 keV. Each data point represents the one-day average of the fitted source fluxes from a number (typically 5–10) of individual ASM dwells, of $\sim$ 90 s each (see Levine et al. 1996

Send offprint requests to: M. Ribó (mribo@mizar.am.ub.es)

[1] The Green Bank Interferometer is a facility of the USA National Science Foundation operated by NRAO in support of the NASA High Energy Astrophysics programs.

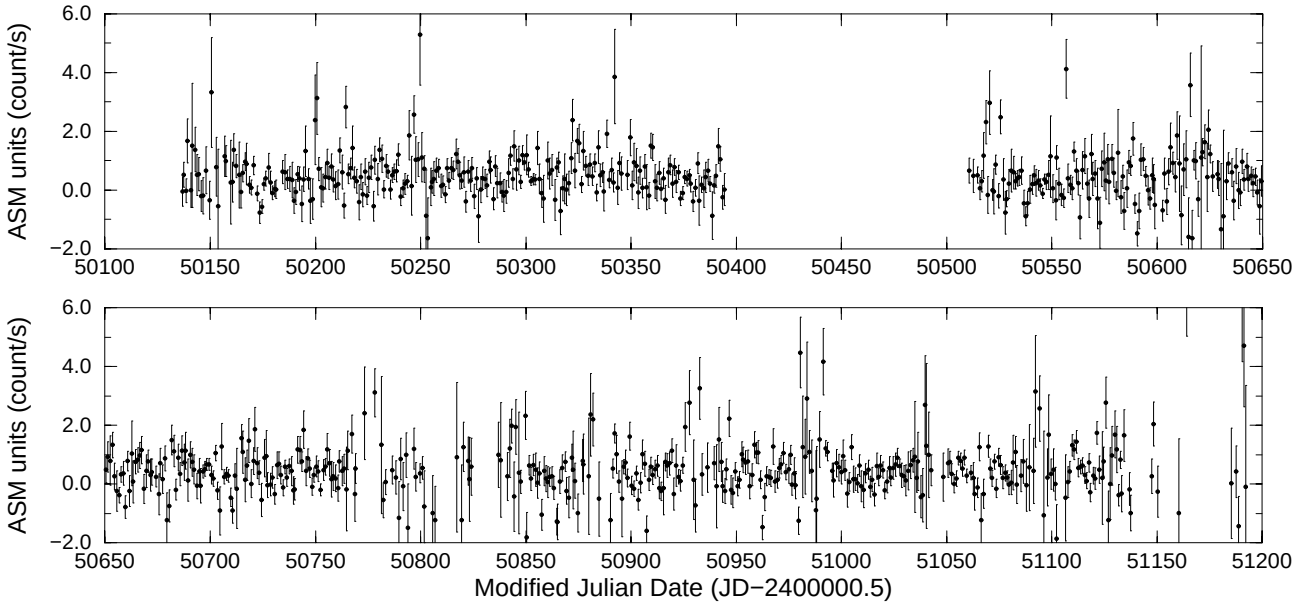

Fig. 1. ASM one-day average light curve of RX J1826.2−1450 in the 1.5–12 keV energy band.

Table 1. Log of the PCA observation of RX J1826.2−1450

Date	Start time (TT)	Stop time (TT)	Luminosity[a] (erg s^{-1})
08/02/98	01:05:33	04:18:14	6.4×10^{34}
08/02/98	20:07:34	00:57:14	5.3×10^{34}
16/02/98	18:42:25	20:35:14	5.3×10^{34}

[a] in the energy range 3–30 keV and for an assumed distance of 3.1 kpc

for more details). The one-day average light curve is shown in Fig. 1. The big gap between Modified Julian Date (MJD) $\sim$ 50400 and $\sim$ 50500 corresponds to the passage of the Sun close to the source during the first year of observations. This gap repeats the following two years (near MJD 50800 and 51150), but it happens to be less severe and a few flux measurements were then possible.

Most of time, the source is at the threshold of ASM detectability. Nevertheless, we have searched for possible periodicities in the range from 2 to 200 d. The methods employed were the Phase Dispersion Minimization (PDM) (Stellingwerf 1978) and the CLEAN algorithm (Roberts et al. 1987). Our approach here is essentially the same as in Paredes et al. (1997) when analyzing the periodic behavior in the X-ray light curve of LS I+61°303.

After applying both the PDM and CLEAN methods to the ASM data, a period of $\sim$ 52.7 d stands prominently. This periodicity corresponds to the detection of some kind of active events that appear rather evident at first glance in Fig. 1. Nevertheless, a careful inspection of the data reveals a suspicious detail. All those active events take place when the data by dwell coverage is rather poor (less than 5 dwells per day), thus reducing the statistical significance of the corresponding one-day average. For some instrumental reason, the ASM coverage becomes poorer than normal every $\sim$ 53 d or so and, in the case of a weak X-ray source like RX J1826.2−1450, this can affect somehow the period analysis. Therefore, the $\sim$ 52.7 d period is very likely to be an instrumental artifact. Indeed, after removing all daily points resulting from less than 5 dwells ($\sim$ 20% of total), the timing analysis reveals no significant period in the range from 2 to 200 d.

2.2. The PCA/RXTE data

Additional observations were made with the PCA instrument on 1998 February 8 and 16. The total on-source integration time was 20 ks. The PCA is sensitive to X-rays in the energy range 2–60 keV and comprises five identical co-aligned gas-filled proportional counter units (PCUs), providing a total collecting area of $\sim$ 6500 cm^2, an energy resolution of $<$ 18% at 6 keV and a maximum time resolution of 1 μs. Our analysis was carried out in the interval 3–30 keV since the PCU windows prevent the detection of photons below $\sim$ 2.5 keV, whereas above 30 keV the spectrum becomes background dominated.

Good time intervals were defined by removing data taken at low Earth elevation angle ($< 8°$) and during times of high particle background. An offset of only 0.02° between the source position and the pointing of the satellite was allowed, to ensure that any possible short stretch of slew data at the beginning and/or end of the observation was removed. Table 1 shows the journal of the PCA observations, while the light curve of the entire observation is presented in Fig. 2.

The PCA observations were used to study the time variability on various time scales. Continuous stretches of clean data were selected from the light curve of the entire observation. To reduce the variance of the noise powers, these intervals were divided up into segments of 8192 bins each, with a bin size of 10 ms. Then the power density spectra for each segment were

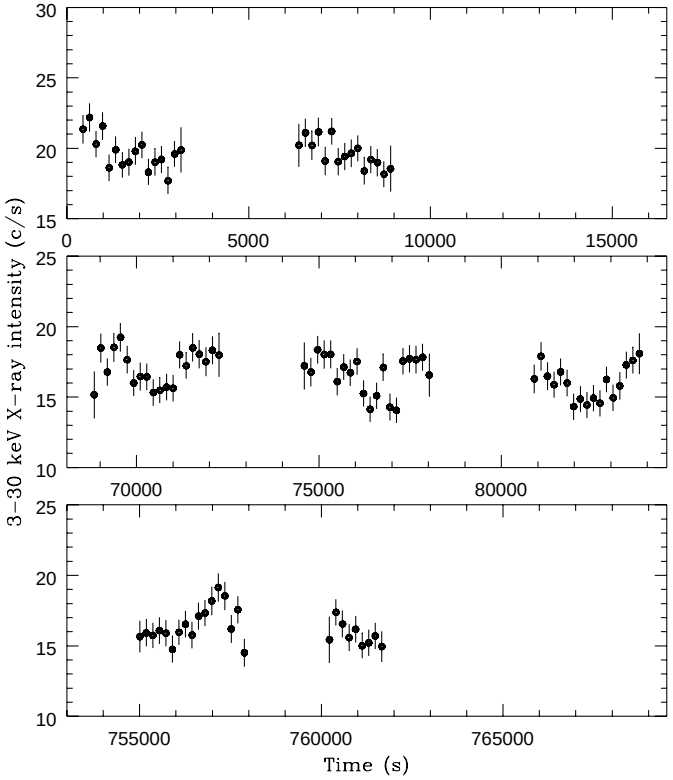

Fig. 2. 3–30 keV light curve of RX J1826.2−1450 covering the entire PCA observation. Time 0 is JD 2 450 853.047 and the bin size is 180 s

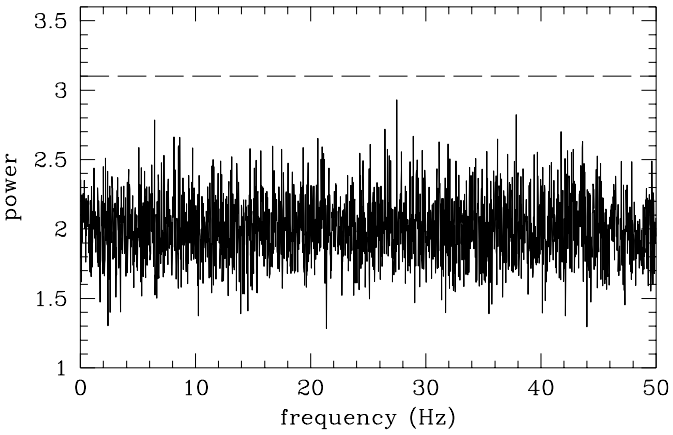

Fig. 3. Characteristic power spectrum of RX J1826.2−1450. The dashed line represents the 95% confidence detection limit

calculated and the results averaged together. Fig. 3 shows the characteristic power spectrum in the frequency range 0.01–50 Hz. The dashed line represents the 95% confidence detection limit (van der Klis 1989). As it can be seen no power exceeds this value; the distribution of powers is flat at a level of 2, consistent with Poissonian counting statistics. Following van der Klis (1989), we can set a 95% upper limit of 60% on the *rms* of a pulsed source signal in the range 0.01–50 Hz. This relatively high limit is a consequence of the faintness of the source. On longer time scales, longer intervals ($\sim$ 3200 s) were considered but no evidence for pulsations was found either.

Table 2. Spectral fit results for the power-law model plus a Gaussian component for the iron line. Uncertainties are given 90% confidence for one parameter of interest. The spectrum was fitted in the energy range 3–30 keV

Parameters	Fitted values
$N_{\rm H}$ ($\times 10^{21}$ cm^{-2})	2^{+1}_{-2}
α	1.95±0.02
$E_{\rm line}$(Fe) (keV)	6.62±0.04
$EW_{\rm line}$(Fe) (keV)	0.75±0.06
$FWHM_{\rm line}$(Fe) (keV)	0.9±0.2
$\sigma_{\rm line}$(Fe) (keV)	0.39±0.08
χ^2_r (dof)	1.14 (56)

Likewise, we folded the light curve onto a set of trial periods with the FTOOLS software package (a technique very similar to the PDM) and looked for a peak in the χ^2 *versus* period diagram. None of the peaks found were statistically significant enough. Thus, we conclude that no coherent periodicities were detected in the range $\sim$ 0.02 to $\sim$ 2000 s.

The mean X-ray intensity in the energy range 3–30 keV shows a slight decreasing trend with 19.7±0.2 count s^{-1} at the beginning of the observation (upper panel of Fig. 2) compared to 16.6±0.1 count s^{-1} and 16.2±0.2 count s^{-1} for the middle and bottom panels of Fig. 2, respectively. The fractional rms of the 3–30 keV light curve corresponding to the entire observation is 9%.

The fact that no X-ray pulsations have been found in RX J1826.2−1450 is consistent with the proposed idea that radio emission and X-ray pulsations from X-ray binaries seem to be statistically anti-correlated (Fender et al. 1997), i.e., no X-ray pulsar has ever shown significant radio emission.

3. X-ray spectral analysis

3.1. Spectral fitting

Since the light curve of the entire observation does not show sharp features, i.e., there is no significant spectral change throughout the observation, we obtained one average PCA energy spectrum from the complete observation (Fig. 4).

Acceptable fits of the X-ray continuum were obtained with an unabsorbed power-law model, giving a reduced χ^2=1.14 for 56 degrees of freedom (dof). A multi-colour disk model, as expected from an optically thick accretion disk (Mitsuda et al. 1984) plus a power-law gave a reduced χ^2_ν=1.11 for 53 dof. The best-fit results are given in Table 2. Bremsstrahlung and two blackbody component models did not fit the data. Although the addition of a blackbody component to the power-law formally produces an acceptable fit, the value of the blackbody normalization was very low, with the error bar close to zero. In fact, an F-test shows that the inclusion of a blackbody component is not significant.

The most salient feature that appears in the spectrum of RX J1826.2−1450 is a strong iron line at $\sim$ 6.6 keV (Fig. 4). A Gaussian fit to this feature gives a line cen-

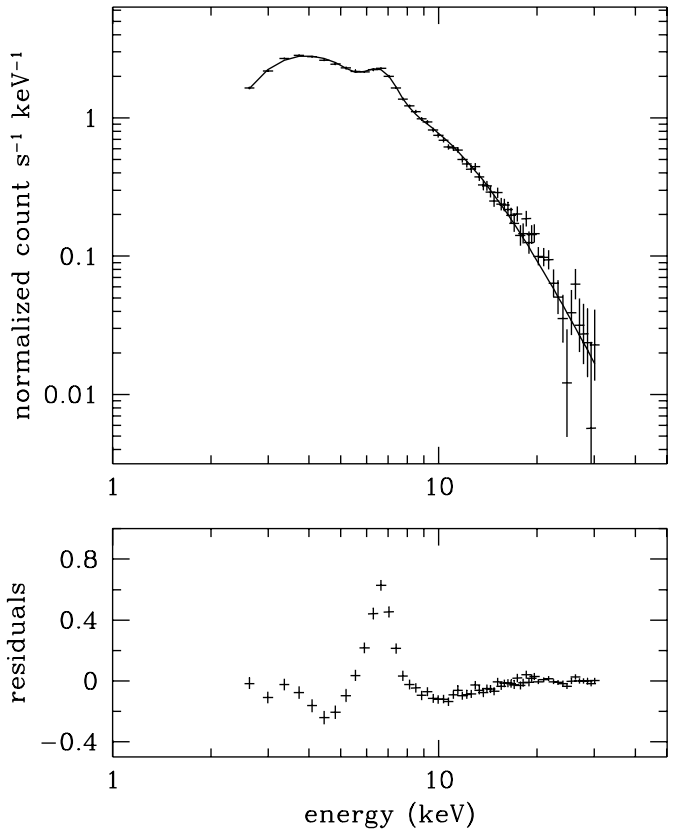

Fig. 4. PCA spectrum of RX J1826.2−1450. The continuous line represents the best-fit power-law model plus a Gaussian component for the iron line. When this component is omitted the line shows up clearly in the residuals

tered at 6.62±0.04 keV, with an equivalent width (EW) of 0.75±0.06 keV and a $FWHM$ of 0.9±0.2 keV. The high EW(Fe) value indicates that a large amount of circumstellar matter is present in the system. Unfortunately, the PCA energy resolution prevents from distinguishing between a broad line or two narrow components.

A hydrogen column density of $\sim (2^{+1}_{-2}) \times 10^{21}$ cm^{-2} is found from the fit. This value is, however, not very well constrained. In fact, it is consistent with zero. The difficulty in constraining the hydrogen column density from our X-ray data can be attributed to the fact that the interstellar gas mainly absorbs X-ray photons with energies lower than 2–3 keV, i.e., outside of the energy range considered here. Nevertheless, it agrees with the value obtained from optical observations. From the λ 4430 and λ 6284 interstellar bands M97 found $E(B-V)$ = 0.8±0.2. Using the relation $N_{\rm H}$ = 5.3 × 10^{21} cm^{-2} $E(B-V)$ (Predehl & Schmitt 1995), we obtain that $N_{\rm H} \sim (4\pm1) \times 10^{21}$ cm^{-2}, which is consistent, within the errors, with the X-ray observation value.

3.2. A black hole or a neutron star?

As mentioned above, no pulsations are found in the X-ray flux of RX J1826.2−1450/LS 5039. At the time of writing this paper approximately 55% of the optically identified massive X-ray binary systems are pulsars, rising to 67% if suspected HMXRB are included. About 75% of the identified and suspected X-ray pulsars have spin periods below 100 seconds. The detection of pulsations would rule out a black hole companion.

Interestingly, unlike typical X-ray pulsars, the energy spectrum of RX J1826.2−1450 shows no exponential cut-off at high energy despite that significant emission is seen up to 30 keV. The absence of both, pulsations and high energy cut-off may indicate that the compact companion is a black hole rather than a neutron star. The persistent non-thermal radio emission of RX J1826.2−1450/LS 5039 is also reminiscent, among others, of the classical black hole candidate (BHC) Cygnus X-1. However, the data are not conclusive as counter-examples of these properties can be found. For example, the system LS I+61°303, which seems to contain a neutron star and does not exhibit pulsations or cut-off in the 10–30 keV range. The multi-colour disk model, although formally fitting the data, does not help either. First, given the low luminosity ($L_{\rm X} < 10^{35}$ erg s^{-1} in the energy range 2–10 keV) the system would be in the so-called low-state. We would not expect then to detect a strong soft component. Second, the fit provides an unrealistic value of the disk internal radius of $R_{\rm in} \cos^{1/2}(\theta) \sim 0.3$ km. Finally, the lack of detected pulsations may be just due to the faintness of the X-ray emission in view of the rather high upper limit found in Sect. 2.2 for pulsed emission.

Unfortunately, the source is too faint at energies above 30 keV to be detected with the HEXTE instrument. Thus, we cannot confirm from the present data whether the hard tail that characterizes the energy spectrum of BHCs at high energies is indeed present. In any case, the issue of a possible black hole in RX J1826.2−1450/LS 5039 is likely to be set in the future by obtaining a spectroscopic mass function in the optical.

4. Radio observations

4.1. Radio variability properties of LS 5039

The radio observations reported here consist of daily flux density measurements with the GBI within the GBI-NASA Monitoring Program. The source was observed at the frequencies of 2.25 and 8.3 GHz. In Fig. 5, we show the corresponding flux density light curves during the first $\sim$ 4 months of monitoring so far available. The bottom panel displays the spectral index α (where $S_\nu \propto \nu^\alpha$) computed between these two frequencies.

The source was found to be detectable at radio wavelengths throughout all the time. This behavior is better evident at 2.25 GHz where the source is brighter. The average GBI flux densities and their respective *rms* are $S_{2.25\ \rm GHz} = 31(\pm5)$ mJy and $S_{8.3\ \rm GHz} = 14(\pm5)$ mJy. The typical day-to-day variability in the GBI data does not exceed $\sim$ 30%. There may be however some exceptions, such as for example around Modified Julian Date (MJD) 51075, 51086 and 51176. Here, the flux density of LS 5039 seems to have varied by more than a factor of $\sim$ 2 on less than one day. Excluding these episodes, the source never exhibited well defined radio outburst events. In general terms, the observed radio behavior confirms the early suggestions by

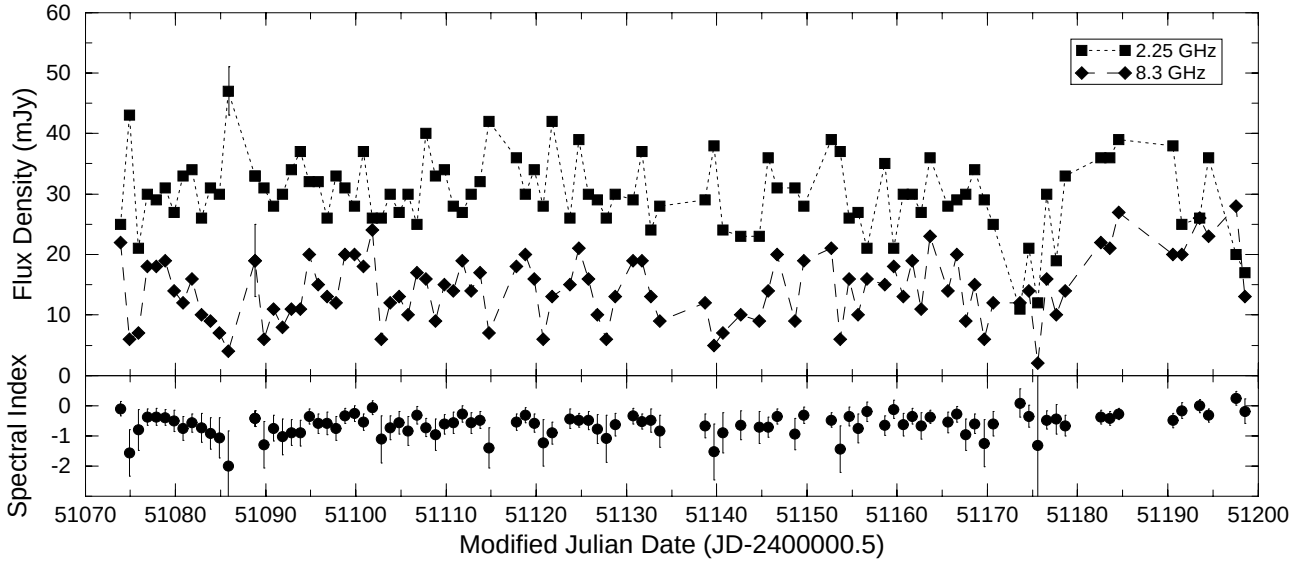

Fig. 5. *Top:* GBI radio light curves of LS 5039 at the frequencies of 2.25 and 8.3 GHz. Representative $\pm$ 1σ error bars have been plotted. *Bottom:* The corresponding spectral index. Error bars are also $\pm$ 1σ. The source behaves as moderately variable and has a clear non-thermal spectral index

Martí et al. (1998) concerning the persistent and moderately variable nature of the radio emission.

Timing analysis of radio light curves has proven to be in some cases a useful tool to detect orbital periods. For example, the orbital period signatures of 26.5 and 5.6 d are visible in LS I+61°303 and Cygnus X-1, respectively (Taylor & Gregory 1984; Pooley et al. 1998). We have thus searched for long-term periodicities in the GBI data of LS 5039. Given the span of the radio observations, the search was restricted between 2 and 50 d. The methods used were again the PDM and CLEAN, mentioned in Sect. 2.1. Unfortunately, no convincing period was detected in this process. A longer time span is likely to be required before a reliable search can be attempted for this relatively weak radio source (specially at 8.3 GHz).

4.2. Non-thermal radio spectrum and brightness temperature

From the GBI data, the weighted average spectral index is found to be $\alpha = -0.5^{+0.2}_{-0.3}$. This value is also in good agreement with the results by Martí et al. (1998) obtained a few months before, thus suggesting that the non-thermal radio spectrum is a persistent property of the source.

In addition to negative spectral indices, the brightness temperature estimates for LS 5039 clearly yield to non-thermal values, hence supporting the mechanism of synchrotron radiation for that source. The apparent one-day variability observed in the GBI data around MJD 51075, 51086 and 51176 would imply, from light time travel arguments, that the emitting region is smaller than about 2.6×10^{15} cm. If we assume a 3.1 kpc distance to the source, the corresponding angular size is found to be $\theta \leq 0\farcs05$, yielding a lower limit of $T_b \geq 6 \times 10^6$ K (at 2.25 GHz). This lower limit is not far from the $T_b \geq 4 \times 10^6$ K estimate by Martí et al. (1998), based on the unresolved nature of the source with the VLA.

5. Comparison to other radio loud HMXRB

SS 433, LS I+61°303 and the BHC Cygnus X-1 are classical examples of HMXRB with detectable radio emission (Penninx 1989), and all of them are also under GBI monitoring. In order to facilitate the comparison of LS 5039 to these sources, we have summarized some relevant parameters in Table 3. They include: the quiescent X-ray luminosity, as derived from ASM/RXTE data (extrapolated from PCA/RXTE in the case of LS 5039 because the signal to noise ratio is much higher); the weighted average radio luminosity and spectral index in quiescence, both based on GBI data; the nature of the compact object; the spectral type of the companion; the orbital period of the binary system and the distance to the source.

As it can be seen in Table 3, the radio luminosity of LS 5039 is very similar to that of Cygnus X-1. This is, of course, provided that the distance adopted is correct. Their respective spectral indices seem to be intrinsically different, both sources being persistent at radio wavelengths. Cygnus X-1 also experiences strong X-ray variability due to changes in its state, that we are not aware of in our source. The LS I+61°303 radio properties during quiescence are also very comparable to those of LS 5039, as well as their respective X-ray luminosities. In contrast, LS I+61°303 undergoes radio outbursts every $\sim$ 26.5 d, the orbital period of the system, while LS 5039 never had strong outbursts during the GBI observations. The X-ray and radio luminosities of SS 433 in quiescence are much higher than those of LS 5039. However, we notice that their $L_{\rm rad}/L_{\rm X}$ ratios are practically the same.

In general terms, the average properties of LS 5039 do not deviate extraordinarily from those of other radio loud HMXRB. Since even the well accepted members of this class are not an homogeneous group, the belonging of LS 5039 to this category appears as very plausible to us.

Table 3. Average properties of radio emitting HMXRBs from ASM/RXTE and GBI data

HMXRB	$L_{\rm X}$(1.5–12 keV) (erg s^{-1})	$L_{\rm rad}$(0.1–100 GHz) (erg s^{-1})	α ($S_\nu \propto \nu^\alpha$)	Compact object	Companion	Orbital period (d)	Distance (kpc)
LS 5039	$\sim 5 \times 10^{34}$	1.0×10^{31}	-0.5	?	O7 V((f))	?	3.1[a]
Cygnus X-1	$\sim 8 \times 10^{36}$ (*)	1.1×10^{31}	0.1	black hole	O9.7 Iab	5.6	2.5[b]
LS I+61°303	$\sim 4 \times 10^{34}$	0.9×10^{31} (*)	-0.3 (*)	neutron star?	B0Ve	26.5	2.0[c]
SS 433	$\sim 7 \times 10^{35}$ (*)	3.2×10^{32} (*)	-0.7 (*)	neutron star?	OB?	13.1	4.8[d]

(*) Only data during quiescence has been considered
[a] Motch et al. 1997
[b] Penninx 1989
[c] Frail & Hjellming 1991
[d] Vermeulen et al. 1993

6. Conclusions

We have presented a general overview of the X-ray and radio emission properties of the massive X-ray binary RX J1826.2−1450/LS 5039. Our X-ray and radio results are mostly based on long term (few months) monitorings of the source, with our main conclusions being:

1. In the X-rays, a timing analysis has been performed showing neither pulsed nor periodic emission on time scales of 0.02–2000 s and 2–200 d, respectively. The X-ray spectrum has been found to be significantly hard (up to 30 keV), with no cut-off required. It can be fitted satisfactorily with a power-law plus a strong Gaussian iron line.
2. At radio wavelengths, the GBI monitoring confirms the long-term persistence of the RX J1826.2−1450/LS 5039 radio emission in time scales of months, always with a non-thermal synchrotron spectrum. The day-to-day variability continues to be moderate most of the time ($\lesssim 30\%$), and no strong radio outbursts have been observed.
3. The classification of RX J1826.2−1450/LS 5039 among the radio loud HMXRB group is reinforced. Although some specific differences with other members of this class do exist, noticeable similarities can be found.

Acknowledgements. We thank Ron Remillard for useful discussion about the ASM data. We also thank Iossif Papadakis for his help in the timing analysis of the PCA data. This paper is partially based on quick-look results provided by the ASM/RXTE team and data obtained through the HEASARC Online Service of NASA/GSFC. We acknowledge detailed and useful comments from an anonymous referee. M.R. is supported by a fellowship from CIRIT (Generalitat de Catalunya, ref. 1999 FI 00199). P.R. acknowledges support via the European Union Training and Mobility of Researchers Network Grant ERBFMRX/CP98/0195. J.M. is partially supported by Junta de Andalucía (Spain). J.M.P and J.M. acknowledge partial support by DGICYT (PB97-0903).

References

Fender R.P., Roche P., Pooley G.G., et al., 1997, Proceedings 2nd INTEGRAL Workshop: The Transparent Universe. ESA SP-382, 303
Frail D., Hjellming R.M., 1991, AJ 101, 2126
Levine A.M., Bradt H., Cui W., et al., 1996, ApJ 469, L33
Martí J., Paredes J.M., Ribó M., 1998, A&A 338, L71
Mitsuda K., Inoue H., Koyama K., et al., 1984, PASJ 36, 741
Motch C., Haberl F., Dennerl K., Pakull M., Janot-Pacheco E., 1997, A&A 323, 853 (M97)
Paredes J.M., Martí J., Peracaula M., Ribó M., 1997, A&A 320, L25
Penninx W., 1989, Proc. 23rd ESLAB Symp. on: Two-Topics in X-Ray Astronomy. ESA SP-296, 185
Pooley G.G., Fender R.P., Brocksopp C., 1998, MNRAS 302, L1
Predehl P., Schmitt J.H.M.M., 1995, A&A 293, 889
Roberts D.H., Lehar J., Dreher J.W., 1987, AJ 93, 968
Stellingwerf R.F., 1978, ApJ 224, 953
Taylor A.R., Gregory P.C., 1984, ApJ 283, 273
van der Klis M., 1989. In: Ögelman H., van den Heuvel E.P.J. (eds.) Timing Neutron stars. Kluwer, Dordrecht, p. 27
Voges W., Boller Th., Dennerl K., et al., 1996, MPE Report 263, 637
Vermeulen R.C., Schilizzi R.T., Spencer R.E., Romney J.D., Fejes I., 1993, A&A 270, 177